Quantification of complementarity in multiqubit systems

Xinhua Peng,[1,2] Xiwen Zhu,[2] Dieter Suter,[1] Jiangfeng Du,[3] Maili Liu,[2] and Kelin Gao[2]
[1]*Fachbereich Physik, Universität Dortmund, 44221 Dortmund, Germany*
[2]*Wuhan Institute of Physics and Mathematics, Chinese Academy of Sciences, Wuhan 430071, People's Republic of China*
[3]*Hefei National Laboratory for Physical Sciences at Microscale and Department of Modern Physics, University of Science and Technology of China, Hefei, Anhui 230026, People's Republic of China*
(Received 28 February 2005; published 16 November 2005)

Complementarity was originally introduced as a qualitative concept for the discussion of properties of quantum mechanical objects that are classically incompatible. More recently, complementarity has become a *quantitative* relation between classically incompatible properties, such as the visibility of interference fringes and "which-way" information, but also between purely quantum mechanical properties, such as measures of entanglement. We discuss different complementarity relations for systems of two-, three-, or n qubits. Using nuclear magnetic resonance techniques, we have experimentally verified some of these complementarity relations in a two-qubit system.

DOI: 10.1103/PhysRevA.72.052109 PACS number(s): 03.65.Ta, 03.65.Ud, 76.60.−k

I. INTRODUCTION

Complementarity is one of the most characteristic properties of quantum mechanics, which distinguishes the quantum world from the classical one. In 1927, Bohr [1] first reviewed this subject, observing that the wavelike and particlelike behaviors of a quantum mechanical object are mutually exclusive in a single experiment, and referred to this as complementarity. Probably the most popular representation of Bohr complementarity is the "wave-particle duality" [2,3], which is closely related to the long-standing debate over the nature of light [4]. This type of complementarity is often illustrated by means of two-way interferometers: A classical particle can take only one path, while a classical wave can pass through both paths and therefore display interference fringes when the two partial waves are recombined. Depending on their state, quantum mechanical systems (quantons) can behave like particles (go along a single path), like waves (show interference), or remain in between these extreme cases by exhibiting particlelike as well as wavelike behavior. This can be quantified by the predictability P, which specifies the probability that the system will go along a specific path, and the visibility V of the interference fringes after recombination of the two partial waves, which quantifies the wavelike behavior. A quantitative expression for the complementarity is the inequality [5–10]

$$P^2 + V^2 \leqslant 1, \tag{1}$$

which states that the more particlelike a system behaves, the less pronounced the wavelike behavior becomes.

In composite systems, consisting of two (or more) quantons, it is possible to optimize the "which-way" information of one particle: one first performs an ideal projective measurement on the second particle. By an appropriate choice of the measurement observable, one can then maximize the predictability for the first partial system. This optimized property, which is called distinguishability D, obeys a similar inequality [5–10]:

$$D^2 + V^2 \leqslant 1. \tag{2}$$

For pure states, the limiting equality holds,

$$D^2 + V^2 = 1, \tag{3}$$

while the inequality holds for mixed states. This issue has been experimentally investigated in the context of interferometric experiments, using a wide range of physical objects including photons [11], electrons [12], neutrons [13], atoms [14], and nuclear spins in a bulk ensemble with nuclear magnetic resonance (NMR) techniques [15,16].

In systems of strongly correlated pairs of particles, it is often useful to consider particle pairs as composite particles with an independent identity. Such composite particles that consist of identical particles include pairs of electrons (Cooper pairs) and photon pairs [17]. Many interesting phenomena, such as superconductivity, are much easier to understand in terms of the composite particles than in terms of the individual particles. Suitable experiments, such as two-photon interference [17,18] can measure properties of the composite particles. These experiments made it possible to quantify the "compositeness" of a two-particle state. Extreme cases are product states, which show no signal in two-particle interference experiments, while maximally entangled states maximize the two-particle visibility but show vanishing visibility in experiments testing the interference of individual particles [19]. Between these extremes lies a continuum of states for which the complementarity relation

$$V_k^2 + V_{12}^2 \leqslant 1 \quad (k = 1,2) \tag{4}$$

holds, which is valid for bipartite pure states [9,20]. Here, V_k is the single-particle visibility for particle k, while V_{12} represents the two-particle visibility. This intermediate regime of the complementarity relation of one- and two-photon interference has only recently been experimentally demonstrated in a Young's double-slit experiment by Abouraddy *et al.* [21].

From a quantum information theoretic point of view, composite quantum systems involve inevitably the concept of entanglement, which is a uniquely quantum resource with

no classical counterpart. Does entanglement constitute a physical feature of quantum systems that can be incorporated into the principle of complementarity? Some authors have explored this question and obtained some important results, such as the complementarities between distinguishability and entanglement [22], between coherence and entanglement [23], and between local and nonlocal information [24], etc. Additionally, some complementarity relations in n-qubit pure systems are also observed such as the relationships between multipartite entanglement and mixedness for special classes of n-qubit systems [25], and between the single-particle properties and the n bipartite entanglements in an arbitrary pure state of n qubits [26].

More recently, Jakob and Bergou [27] derived a generalized duality relation between bipartite and single-partite properties for an arbitrary pure state of two qubits, which in some sense accounts for many previous results. They showed that an arbitrary normalized pure state $|\Theta\rangle$ of a two-qubit system satisfies the expression [27]:

$$C^2 + V_k^2 + P_k^2 = 1. \tag{5}$$

Here the concurrence C [28,29] is defined by

$$C(|\Theta\rangle) \equiv |\langle\Theta|(\sigma_y^{(1)} \otimes \sigma_y^{(2)})|\Theta^*\rangle| \tag{6}$$

as a measure of entanglement. $\sigma_y^{(k)}$ is the y component of the Pauli operator on qubit k and $|\Theta^*\rangle$ is the complex conjugate of $|\Theta\rangle$. The concurrence is a bipartite quantity, which quantifies quantum *nonlocal* correlations of the system and is taken as a measure of the *bipartite* character of the composite system. The complement

$$S_k^2 = V_k^2 + P_k^2 \tag{7}$$

combines the single-particle fringe visibility V_k and the predictability P_k. This quantity is invariant under local unitary transformations (though V_k and P_k are not), and is therefore taken as a quantitative measure of the *single-particle* character of qubit k.

Since the two-particle visibility is equal to the concurrence, $V_{12} \equiv C$ [27], we can rewrite Eq. (5) as

$$V_{12}^2 + V_k^2 + P_k^2 = 1 \quad (k = 1,2). \tag{8}$$

This turns the inequality (4) into an equality and identifies the missing quantity as the predictability P_k.

For pure bipartite systems, an equation similar to Eq. (3) holds $D_k^2 + V_k^2 = 1$. Here, the index $k = 1,2$ refers to the different particles as the interfering objects in the bipartite system. Combining this with Eq. (5), we obtain

$$D_k^2 = P_k^2 + C^2. \tag{9}$$

Apparently, D_k contains both the *a priori* WW information P_k and the additional information encoded in the quantum correlation to an additional quantum system which serves as the possible information storage. This quantum correlation can be measured by the concurrence. This reveals explicitly that quantum correlation can help to optimize the information that can be obtained from a suitable measurement; without entanglement, the available WW information is limited to the *a priori* WW knowledge P_k.

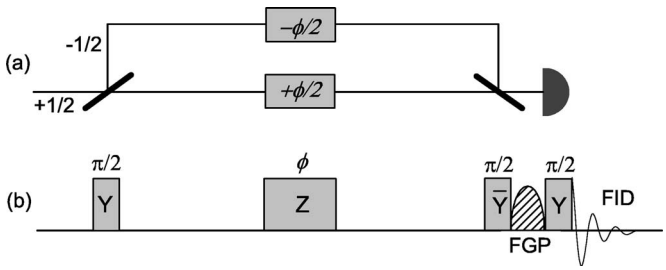

FIG. 1. Principle of NMR interferometry: (a) Path representation and (b) pulse sequence.

For *mixed states*, a weaker statement for the complementarity (5) is found in the form of an inequality $C^2 + V_k^2 + P_k^2 \leqslant 1$. However, there is no corresponding inequality for the two-particle visibility V_{12} in the mixed two-particle sources because it is very difficult to get a clear and definite expression for V_{12} and the direct relation between concurrence and two-particle visibility ceases to exist for mixed states [27].

In this paper, we give a proof-of-principle experimental demonstration of the complementarities (3), (5), and (8) in a two-qubit system. In addition, we extend the complementarity relation (5) to multiqubit systems. The remainder of the paper is organized as follows: In Sec II, we introduce NMR interferometry as a tool for measuring visibilities and which-way information. Sections III and IV discuss measurements of the visibilities and the which-way information in pure bipartite systems. Section V is an experimental investigation of the complementarity relation for a pure bipartite system on the basis of liquid-state NMR. For this purpose, we express the entanglement (concurrence) in terms of directly measurable quantities: the two-particle visibility V_{12} and the distinguishability D_k. This allows us to test two interferometric complementarities (8) and (3) by specific numerical examples. In Sec. VI we generalize the complementarity relation (5) to multiqubit systems. A quantitative complementarity relation exists between the single-particle property and the bipartite entanglement between the particle and the remainder of the system in pure multiqubit systems. This allows us to derive, for pure three-qubit system, a relation between the single-particle, bipartite, and tripartite properties, which should generalize to arbitrary pure states of n qubit systems. Finally, a brief summary with a discussion is given in Sec. VII.

II. NMR INTERFEROMETRY

Complementarity relations are often discussed in terms of photons or other particles propagating along different paths. Another, very flexible approach is to simulate these systems in a quantum computer. In particular liquid state NMR has proved very successful for such investigations. Optical interferometers can readily be simulated by NMR-interferometry [30].

Figure 1 shows how such an interferometric experiment can be implemented by a sequence of radio-frequency pulses. Assuming an ideal spin $I = \frac{1}{2}$ particle, the Hilbert space $\mathcal{H}_1$ associated with the particle is spanned by vectors

$|0\rangle(m=+\frac{1}{2})$ and $|1\rangle(m=-\frac{1}{2})$. A beam splitter, which puts the particle incoming from one port into a superposition of both paths is realized by a radio frequency (rf) pulse that puts the spin in a superposition of the two basis states. If the flip angle of the pulse is taken as $\pi/2$, it corresponds to a *symmetric* beam splitter. A relative phase shift between the two paths, which corresponds to a path length difference, can be realized by a rotation of the spin around the z axis. The second $\pi/2$ radio frequency pulse recombines the two paths.

For the discussion of the complementarity of interference vs which-way information, we consider the superposition state behind the first beam splitter as the starting point. The action of the phase shifter and the second beam splitter can then be summarized into a transducer. Mathematically, this transducer maps the input state into an output state by the transformation

$$U(\phi) = e^{i\pi/4\sigma_y} e^{-i\phi/2\sigma_z} = \frac{1}{\sqrt{2}} \begin{pmatrix} e^{-i\phi/2} & e^{i\phi/2} \\ -e^{-i\phi/2} & e^{i\phi/2} \end{pmatrix}. \quad (10)$$

In the NMR interferometer, a number of different possibilities exist for implementing the action of the transducer. We chose the following pulse sequence, which provides high fidelity for a large range of experimental parameters:

$$[\pi]_{(-\pi-\phi)/2} \left[\frac{\pi}{2}\right]_{\pi/2}. \quad (11)$$

Here, we have used the usual convention that $[\alpha]_\beta$ refers to an rf pulse with flip-angle α and phase β.

The resulting populations of both states in the output space vary with the phase angle ϕ. As shown in Fig. 1, they can be read out by first deleting coherence with a field gradient pulse (FGP) and then converting the population difference into observable transverse magnetization by a $\pi/2$ read-out pulse. The amplitude of the resulting FID (the integral of the spectrum) measures then the populations:

$$S_{NMR} \sim p(|0\rangle) - p(|1\rangle) = 2p(|0\rangle) - 1,$$

where we have taken into account that the sum of the populations is unity. The experimental signal can be normalized to the signal of the system in thermal equilibrium.

Figure 2 shows, as an example, the interference pattern for the single proton spin in H_2O. The amplitude of the spectral line shows a sinusoidal variation with the phase angle ϕ, which implies the sinusoidal variation of the population $p(|0\rangle)$ or $p(|1\rangle)$.

The visibility of the resulting interference pattern is defined as

$$V = \frac{[p(|x\rangle)]_{\max} - [p(|x\rangle)]_{\min}}{[p(|x\rangle)]_{\max} + [p(|x\rangle)]_{\min}}, \quad (12)$$

where $x=0$ or 1, and p_{min} and p_{max} are the minimal and maximal populations (as a function of ϕ).

Since an input state

$$\rho^{(i)} = \tfrac{1}{2}(1 + \vec{s}^{(i)} \cdot \vec{\sigma}) \quad (13)$$

with an initial Bloch vector $\vec{s}^{(i)} = (s_x^{(i)}, s_y^{(i)}, s_z^{(i)})$ and Pauli spin operators $\vec{\sigma} = (\sigma_x, \sigma_y, \sigma_z)$ is transformed into

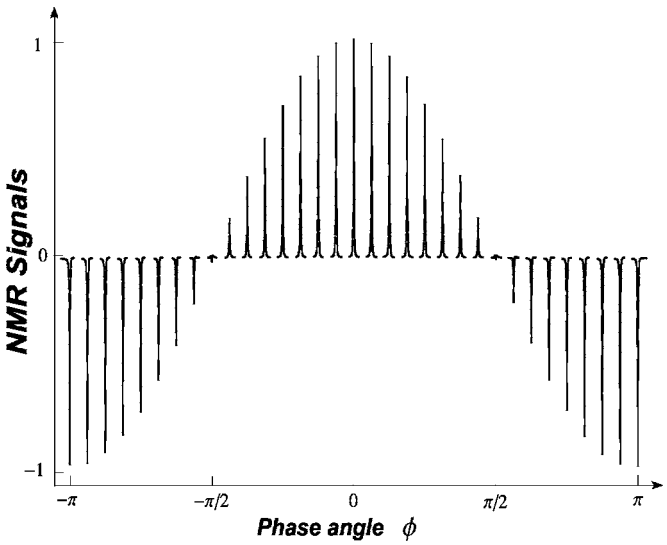

FIG. 2. NMR signals versus the phase angle ϕ.

$$\rho^{(i)} \xrightarrow{U(\phi)} \rho^{(f)} = \tfrac{1}{2}(1 + \vec{s}^{(f)} \cdot \vec{\sigma}) \quad (14)$$

with $\vec{s}^{(f)} = (-s_z^{(i)}, s_x^{(i)} \sin\phi + s_y^{(i)} \cos\phi, s_x^{(i)} \cos\phi - s_y^{(i)} \sin\phi)$ by the transducer, we find for the visibility

$$V = \sqrt{(s_x^{(i)})^2 + (s_y^{(i)})^2} \quad (15)$$

and for the predictability

$$P = |s_z^{(i)}|. \quad (16)$$

With the described experiment, it is thus straightforward to verify the inequality (1).

III. VISIBILITIES IN BIPARTITE SYSTEMS

A. Theory

The NMR interferometry experiment can easily be expanded to multiqubit systems. We start with a discussion of pure bipartite systems, where we explore the visibility in different types of interferometric experiments, geared towards single- and bipartite properties. Figure 3 shows the reference setup: The source **S** emits a pair of particles 1 and 2, one of which propagates along path A and/or A', through a variable phase shifter ϕ_1 impinging on an ideal beam splitter BS_1, and is then registered in either beam K_1 or L_1. On the other side there is the analogous process for the other particle with paths B and B'.

Without loss of the generality, we first associate states $|A\rangle$, $|B\rangle$, $|K_1\rangle$, and $|K_2\rangle$ in Fig. 3 with the spin-up state $|0\rangle$ and

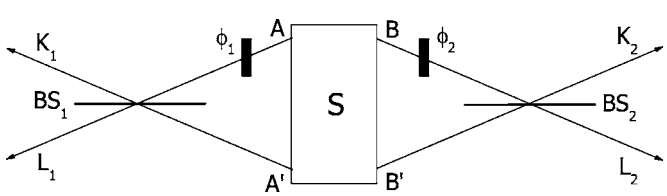

FIG. 3. Schematic two-particle interferometer using beam splitters BS_1, BS_2, and phase shifters ϕ_1, ϕ_2.

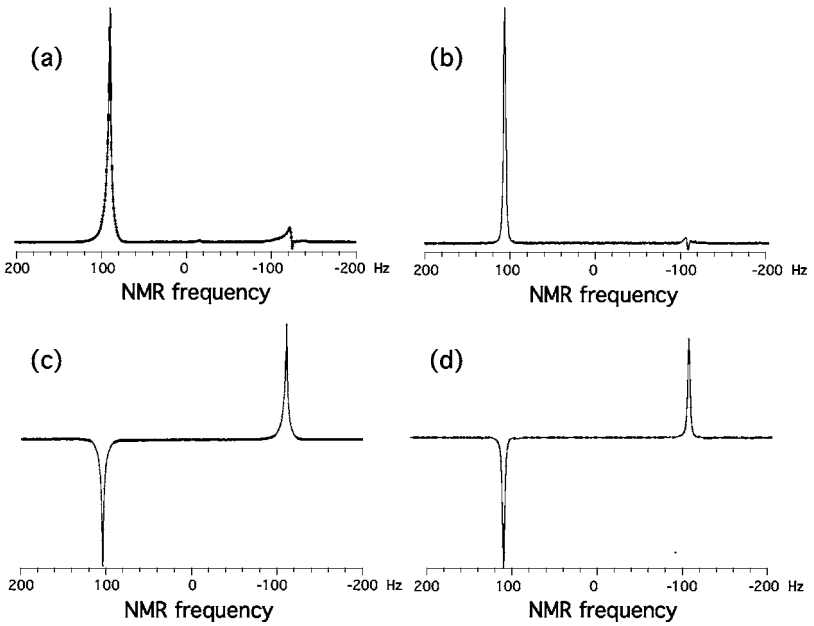

FIG. 4. Experimental spectra of proton and carbon at $\phi_k=0$: (a) and (b) for the product state $|\Phi\rangle$; (c) and (d) for the entangled state $|\Psi\rangle$. (a) and (c) are the proton signals and (b) and (d) are the carbon signals.

$|A'\rangle$, $|B'\rangle$, $|L_1\rangle$, and $|L_2\rangle$ with the spin-down state $|1\rangle$. A particle pair emitted from the source **S** can be expressed as the general pure two-qubit state $|\Theta\rangle$:

$$|\Theta\rangle = \gamma_1|0\rangle_1|0\rangle_2 + \gamma_2|0\rangle_1|1\rangle_2 + \gamma_3|1\rangle_1|0\rangle_2 + \gamma_4|1\rangle_1|1\rangle_2 \tag{17}$$

with complex coefficients γ_i that are normalized to 1.

Assuming that the transducers consist of variable phase shifters and *symmetric* beam splitters, they can be described by the unitary operation

$$\mathcal{U}(\phi_1,\phi_2) = U_1(\phi_1) \otimes U_2(\phi_2), \tag{18}$$

where each transducer is defined according to Eq. (10). Here the subscripts label two different particles. Applying the transducer (18) to the initial state (17), we can calculate the detection probabilities in the output channels as

$$p(|x\rangle_1) = \tfrac{1}{2} + (-1)^x|\gamma_1\gamma_3^* + \gamma_2\gamma_4^*|\cos(\phi_1 - \delta_1),$$

$$p(|x\rangle_2) = \tfrac{1}{2} + (-1)^x|\gamma_1\gamma_2^* + \gamma_3\gamma_4^*|\cos(\phi_2 - \delta_2), \tag{19}$$

where $x=0$ or 1, $\gamma_1\gamma_3^*+\gamma_2\gamma_4^*=|\gamma_1\gamma_3^*+\gamma_2\gamma_4^*|e^{i\delta_1}$, and $\gamma_1\gamma_2^*+\gamma_3\gamma_4^*=|\gamma_1\gamma_2^*+\gamma_3\gamma_4^*|e^{i\delta_2}$. The single-particle count rates $p(|x\rangle_k)$ reach their maxima and minima when the phase shifters are set to $\phi_k=n\pi+\delta_k(n=0,\pm1)$. From Eqs. (12) and (19), the single-particle visibilities can be obtained as

$$\mathcal{V}_1 = 2|\gamma_1\gamma_3^* + \gamma_2\gamma_4^*|, \quad \mathcal{V}_2 = 2|\gamma_1\gamma_2^* + \gamma_3\gamma_4^*|. \tag{20}$$

Two-particle properties can be measured by higher order correlations. Following Refs. 9 and 20, we use the "corrected" two-particle fringe visibility

$$\mathcal{V}_{12} = \frac{[\bar{p}(|x\rangle_1|y\rangle_2)]_{\max} - [\bar{p}(|x\rangle_1|y\rangle_2)]_{\min}}{[\bar{p}(|x\rangle_1|y\rangle_2)]_{\max} + [\bar{p}(|x\rangle_1|y\rangle_2)]_{\min}}. \tag{21}$$

where $x,y=0$ or 1. The corrected joint probability $\bar{p}(|x\rangle_1|y\rangle_2)=p(|x\rangle_1|y\rangle_2)-p(|x\rangle_1)p(|y\rangle_2)+\frac{1}{4}$ are defined such that single-particle contributions are eliminated [9,20]. $p(|x\rangle_1|y\rangle_2)$ denotes the probabilities of joint detections. As the visibilities explicitly depend on the form of the transducers involved and the details of the measurement (e.g., the measurement basis $\{|K\rangle,|L\rangle\}$ is chosen as $\{|0\rangle,|1\rangle\}$), we use the symbols $\mathcal{V}_k$, $\mathcal{V}_{12}$ here, to indicate the experimental visibilities under a specific experimental configuration, as opposed to the maximal visibilities V_k, V_{12}.

The corrected two-particle joint probabilities can be calculated as

$$\bar{p}(|x\rangle_1|y\rangle_2) = \tfrac{1}{4}\{1 + (-1)^{x+y}[|M|\cos(\phi_1 + \phi_2 - \xi_1) + |N|\cos(\phi_1 - \phi_2 - \xi_2)]\}, \tag{22}$$

where

$$M = \gamma_1\gamma_4^* - (\gamma_1\gamma_3^* + \gamma_2\gamma_4^*)(\gamma_1\gamma_2^* + \gamma_3\gamma_4^*) = |M|e^{i\xi_1},$$

$$N = \gamma_2\gamma_3^* - (\gamma_1\gamma_3^* + \gamma_2\gamma_4^*)(\gamma_1^*\gamma_2 + \gamma_3^*\gamma_4) = |N|e^{i\xi_2}. \tag{23}$$

The maximal and minimal values of $\bar{p}(|x\rangle_1|y\rangle_2)$ are thus

$$\bar{p}_{\max,\min}(|x\rangle_1|y\rangle_2) = \tfrac{1}{4}[1 \pm 2(|M| + |N|)]. \tag{24}$$

These values are reached only when the phase shifters are set to $(\phi_1,\phi_2)=(n\pi+(\xi_1+\xi_2)/2, m\pi+(\xi_1-\xi_2)/2)$, where the parameters n,m can be $(n,m=0,\pm1)$. Hence, on substituting for the maximal and minimal values of these probabilities in Eq. (21), we find

$$\mathcal{V}_{12} = 2(|M| + |N|). \tag{25}$$

With Eqs. (20), (23), and (25), the complementarity relation (4) is obtained, valid for arbitrary pure bipartite states.

B. Experiments on two extreme cases

For the experimental measurements, we used the nuclear spins of ^{13}C-labeled chloroform as a representative two-qubit

quantum system. We identified the spin of the ^{1}H nuclei with particle 1 and the carbon nuclei (^{13}C) with particle 2. The spin-spin coupling constant J between ^{13}C and ^{1}H is 214.95 Hz. The relaxation times were measured to be $T_1=16.5$ sec and $T_2=6.9$ sec for the proton, and $T_1=21.2$ sec and $T_2=0.35$ sec for the carbon nuclei. Experiments were performed on an Infinity+NMR spectrometer equipped with a Doty probe at the frequencies 150.13 MHz for ^{13}C and at 599.77 MHz for ^{1}H, using conventional liquid-state NMR techniques.

For most of the experiments that we discuss in the following, the system was first prepared into a pseudopure state $\rho_{00}=(1-\epsilon)/(tr(\mathbf{1}))\mathbf{1}+\varepsilon|00\rangle\langle 00|$. Here, $\mathbf{1}$ is the unity operator and ε a small constant of the order of 10^{-5} determined by the thermal equilibrium. We used the spatial averaging technique [31] and applied the pulse sequence:

$$\left[\frac{\pi}{3}\right]^1_{\pi/2} - G_z - \left[\frac{\pi}{4}\right]^1_{\pi/2} - \frac{\pi/2}{\pi J} - \left[\frac{\pi}{4}\right]^1_0 - G_z, \qquad (26)$$

where G_z is a field gradient pulse that destroys the transverse magnetizations. The upper indices of the pulses indicate to which qubit the rotation is applied.

Starting from this pseudopure state, we then prepared the two-particle source states $|\Theta\rangle$. As an example, we consider a product state $|\Phi\rangle$

$$|\Phi\rangle = \left(\frac{1}{\sqrt{2}}(|0\rangle_1 + |1\rangle_1)\right) \otimes \left(\frac{1}{\sqrt{2}}(|0\rangle_2 + |1\rangle_2)\right), \qquad (27)$$

and a maximally entangled state $|\Psi\rangle$

$$|\Psi\rangle = \frac{1}{\sqrt{2}}(|0\rangle_1|0\rangle_2 + |1\rangle_1|1\rangle_2). \qquad (28)$$

They can be prepared from ρ_{00} by the following pulse sequences:

$$|\Phi\rangle: \left[\frac{\pi}{2}\right]^1_{\pi/2}\left[\frac{\pi}{2}\right]^2_{\pi/2},$$

$$|\Psi\rangle: \left[\frac{\pi}{2}\right]^1_0\left[\frac{\pi}{2}\right]^1_{\pi/2}\left[\frac{\pi}{2}\right]^2_{\pi}\left[\frac{\pi}{2}\right]^2_{3\pi/2}\left[\frac{\pi}{2}\right]^2_{\pi/2} - \frac{\pi/2}{\pi J} - \left[\frac{\pi}{2}\right]^2_{\pi/2}, \qquad (29)$$

where $-\theta/\pi J-$ represents a free evolution for this time under the scalar coupling.

The actual interferometer was realized by applying the transducers $\mathcal{U}(\phi_1,\phi_2)$ of Eq. (18) to the prepared state $|\Theta\rangle$, which describes the effect of the phase shifters and symmetric beam splitters. The transducer pulse sequence (11) is simultaneously applied to both qubits.

The probabilities that enter the complementarity relations can be expressed in terms of populations of the four spin states. To determine these spin states, we used a simplified quantum state tomography scheme to reconstruct only the diagonal elements of the density matrix. This was realized by

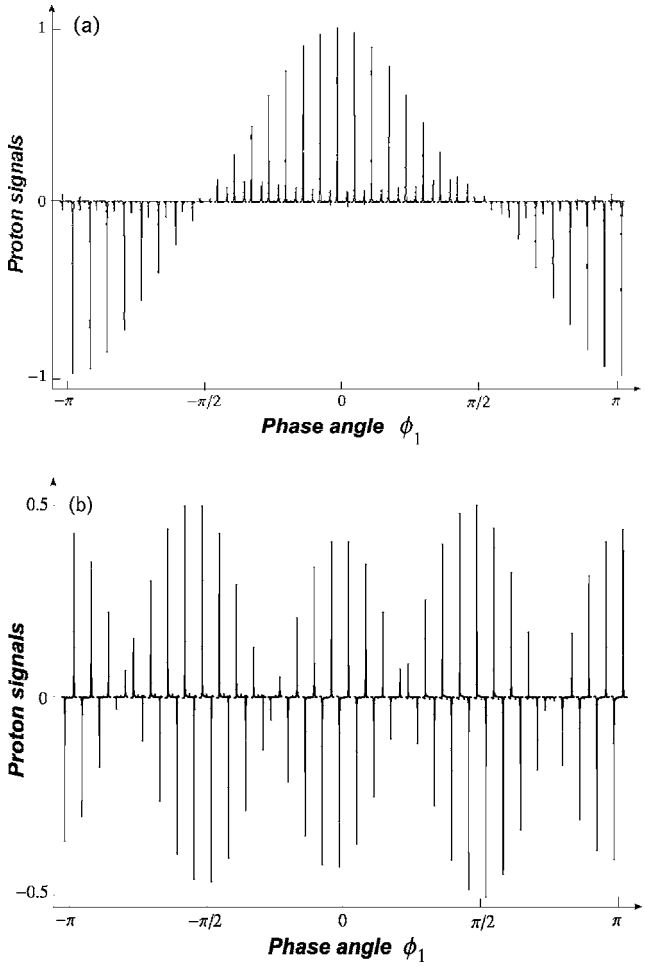

FIG. 5. Experimental spectra of proton with the phase ϕ_1: (a) for the product state $|\Phi\rangle$ and (b) for the entangled state $|\Psi\rangle$.

$$G_z - \left[\frac{\pi}{2}\right]^k_{\pi/2} - \mathrm{FID}_k \qquad (30)$$

for $k=1,2$. FID_k represents to recording the FID of qubit k after a field gradient pulse G_z and a read-out pulse $[\pi/2]^k_{\pi/2}$. Figure 4 shows the NMR signals after Fourier transformation of the corresponding FIDs for the proton and carbon spins in $^{13}CHCl_3$ at $\phi_k=0$ when they are prepared in the product state $|\Phi\rangle$ or the maximally entangled state $|\Psi\rangle$. The signals measure the populations

$$S_{NMR}(\text{Proton}) \sim p(|0\rangle_1|x\rangle_2) - p(|1\rangle_1|x\rangle_2),$$

$$S_{NMR}(\text{Carbon}) \sim p(|x\rangle_1|0\rangle_2) - p(|x\rangle_1|1\rangle_2), \qquad (31)$$

where $x=0$ for the high-frequency resonance line and 1 for the low-frequency line.

To create an interferogram, we varied the phases ϕ_k from 0 to 2π, incrementing both simultaneously in steps of $\pi/16$. The resulting interference pattern of the proton is shown in Fig. 5. The carbon signals have a similar behavior as a function of ϕ_2 for the states $|\Phi\rangle$ and $|\Psi\rangle$, as Fig. 5 shows. From these experimental data points, we calculated the probabilities $p(|x\rangle_k)$ and $\bar{p}(|x\rangle_1|y\rangle_2)$ and fitted those to a cosine func-

tion: $y=A\cos(x-x_0)+B$. From the fitted values of the amplitude A and the offset B, we extracted the experimental visibilities as $\mathcal{V}_1=1.04\pm0.02$, $\mathcal{V}_2=0.99\pm0.01$, $\mathcal{V}_{12}=0.05\pm0.01$ for the product state $|\Phi\rangle$ and $\mathcal{V}_1=0.03\pm0.01$, $\mathcal{V}_2=0.14\pm0.01$, $\mathcal{V}_{12}=0.86\pm0.02$ for the entangled state $|\Psi\rangle$ by the definitions of Eqs. (12) and (21). As theoretically expected, the product state $|\Phi\rangle$ shows one-particle interference fringes, but almost no two-particle interference fringes, while the situation is reversed for the entangled state $|\Psi\rangle$. It can also be seen that the discrepancies from the theory are larger for the entangled state $|\Psi\rangle$ than for the product state $|\Phi\rangle$. This is easily understood by realizing that the state preparation is more complicated for the entangled state.

IV. WHICH-WAY INFORMATION IN BIPARTITE SYSTEMS

A. Predictability

For the same system, we can calculate the predictabilities, i.e. the probabilities for correctly predicting which path the particle will take, from the expectation value of the $\sigma_z^{(k)}$ observable on the state $|\Theta\rangle$, i.e., $\mathcal{P}_k=|\langle\Theta|\sigma_z^{(k)}|\Theta\rangle|$:

$$\mathcal{P}_1=\big||\gamma_1|^2+|\gamma_2|^2-|\gamma_3|^2-|\gamma_4|^2\big|$$

$$\mathcal{P}_2=\big||\gamma_1|^2-|\gamma_2|^2+|\gamma_3|^2-|\gamma_4|^2\big|, \tag{32}$$

where $\sigma_z^{(k)}$ is the z component of the Pauli operator on qubit k. $\mathcal{P}_k$ is thus the magnitude of the difference between the probabilities that particle k takes path $|0\rangle_k$ or the other path $|1\rangle_k$.

For the experimental measurement of the predictability $\mathcal{P}_k$, we measure the observable $\sigma_z^{(k)}$ by partial quantum state tomography: a field gradient pulse destroys coherences and a readout pulse $[\pi/2]_{\pi/2}^k$ converts $\sigma_z^{(k)}$ into $\sigma_x^{(k)}$, which is recorded as the FID. Upon Fourier transformation, the integral of both lines yields $\langle\sigma_z^{(k)}\rangle$, and its magnitude corresponds to the predictability $\mathcal{P}_k$.

Figure 6 shows the measurement of the predictability $\mathcal{P}_2$ on $^{13}CHCl_3$ for two specific examples: the product state

$$|\Phi(\theta)\rangle=\left[\frac{1}{\sqrt{2}}(|0\rangle_1+|1\rangle_1)\right]\otimes\left[\cos\frac{\theta}{2}|0\rangle_2+\sin\frac{\theta}{2}|1\rangle_2\right]$$

and the entangled state

$$|\Psi(\theta)\rangle=\frac{1}{\sqrt{2}}\left\{|0\rangle_1\otimes\left[\frac{1}{\sqrt{2}}(|0\rangle_2+|1\rangle_2)\right]+|1\rangle_1\otimes\left[\cos\frac{\theta}{2}|0\rangle_2+\sin\frac{\theta}{2}|1\rangle_2\right]\right\}.$$

B. Distinguishability

In a bipartite system, the which-way information for particle k can be optimized by first performing a projective measurement on particle $j(j\neq k)$. For this measurement, we first have to choose the optimal ancilla observable $W_j^{(opt)}$. According to Englert's quantitative analysis of the distinguishability

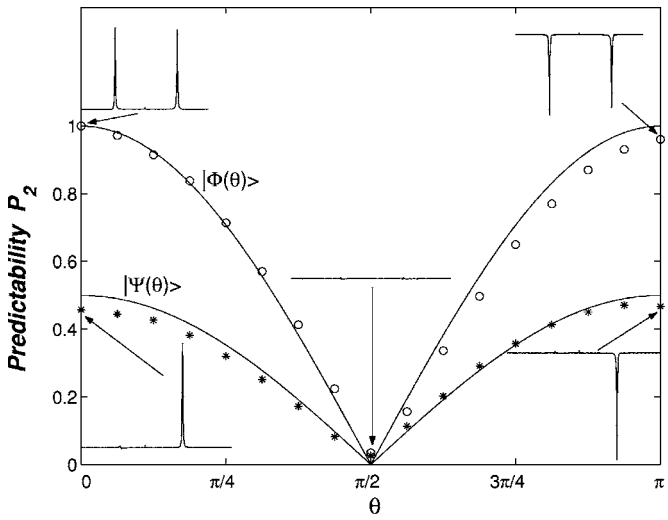

FIG. 6. Experimental meaurement of the predictability $\mathcal{P}_2$ for $|\Phi(\theta)\rangle$ (denoted by ○) and $|\Psi(\theta)\rangle$ (denoted by ∗). The solid lines are the theoretical expectations. The insets are, respectively, the experimental spectra at $\theta=0,\pi/2,\pi$.

[10], we start by writing the quantum state $|\Theta\rangle$ as the sum of two components corresponding to two paths of qubit k:

$$|\Theta\rangle=a_{k+}|0\rangle_k|m_+\rangle_j+a_{k-}|1\rangle_k|m_-\rangle_j. \tag{33}$$

Each component is coupled to a different state of qubit j:

$$|m_+\rangle_j=\frac{\gamma_1}{a_{k+}}|0\rangle_j+\frac{\gamma_{1+k}}{a_{k+}}|1\rangle_j,$$

$$|m_-\rangle_j=\frac{\gamma_{4-k}}{a_{k-}}|0\rangle_j+\frac{\gamma_4}{a_{k-}}|1\rangle_j. \tag{34}$$

The coefficients $a_{k\pm}$ are

$$a_{k+}=\sqrt{|\gamma_1|^2+|\gamma_{1+k}|^2},$$

$$a_{k-}=\sqrt{|\gamma_{4-k}|^2+|\gamma_4|^2}. \tag{35}$$

A suitable measurement is performed on qubit j to make qubit k acquire the maximal which-way information. To determine the most useful ancilla observable, we write it as $W_j=\vec{b}\cdot\vec{\sigma}^{(j)}$. The probability that the ancilla observable finds eigenvalue λ differs for the two component states:

$$p_+(\lambda)=a_{k+}^2\langle\psi_\lambda|(|m_+\rangle_j\langle m_+|_j)|\psi_\lambda\rangle,$$

$$p_-(\lambda)=a_{k-}^2\langle\psi_\lambda|(|m_-\rangle_j\langle m_-|_j)|\psi_\lambda\rangle, \tag{36}$$

where ψ_λ is the corresponding eigenvector.

The distinguishability D_k for qubit k is obtained by maximizing the difference of the measurement probabilities for the two components,

$$D_k=\max\left\{\sum_\lambda|p_+(\lambda)-p_-(\lambda)|\right\}. \tag{37}$$

Using the notation

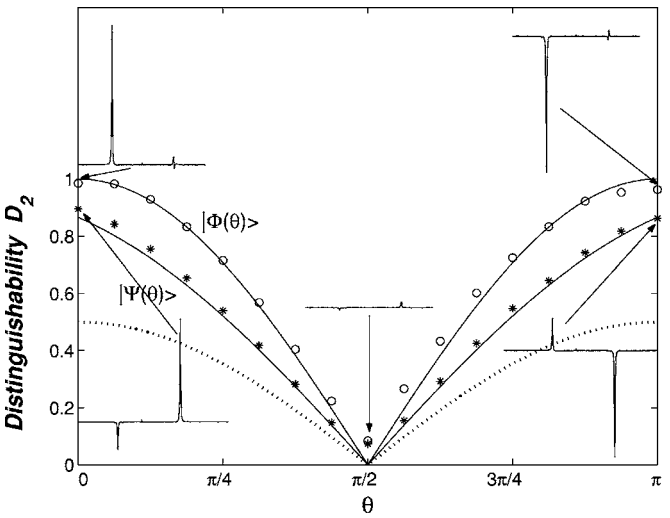

FIG. 7. Experimental meaurement of the distinguishability D_2 for $|\Phi(\theta)\rangle$ (denoted by ○) and $|\Psi(\theta)\rangle$ (denoted by ∗). The solid lines are the theoretical expectations and the dotted line is the theoretical expectation of the predictability $\mathcal{P}_2$ for $|\Psi(\theta)\rangle$. The insets are, respectively, the experimental spectra at $\theta=0,\pi/2,\pi$.

$$|m_\pm\rangle\langle m_\pm| = \vec{m}_\pm \cdot \vec{\sigma}, \tag{38}$$

where $\vec{m}_\pm$ are vectors on the Bloch sphere, we write

$$D_k = \max\{|\vec{b}\cdot[a_{k+}^2\vec{m}_+ - a_{k-}^2\vec{m}_-]|\}. \tag{39}$$

Clearly the maximum is reached if the two vectors $\vec{b}$ and $[a_{k+}^2\vec{m}_+ - a_{k-}^2\vec{m}_-]$ are parallel. Since $\vec{b}$ has unit length, the distinguishability becomes

$$D_k = \|a_{k+}^2\vec{m}_+ - a_{k-}^2\vec{m}_-\| = \sqrt{1-2a_{k+}^2a_{k-}^2(1+\vec{m}_+\cdot\vec{m}_-)}. \tag{40}$$

Combining Eqs. (20) and (40), we obtain the complementarity relation (3), i.e., $D_k^2+V_k^2=1$ for $k=1,2$.

For the experimental measurement, we first have to perform a "measurement" on the ancilla qubit j, using the optimal observable $W_j=\vec{b}\cdot\vec{\sigma}_j$. This is done by applying a unitary transformation R to rotate the eigenbasis $\{|\psi_\lambda\rangle_j\}$ of the observable $W_j^{(opt)}$ into the computational basis $\{|0\rangle_j,|1\rangle_j\}$ [32]. The subsequent field gradient pulse destroys coherence of qubit j [33], as well as qubit k and joint coherences (=zero and double quantum coherences). After this ancilla measurement, the distinguishability D_k can be measured by a readout pulse, detection of the FID, Fourier transformation, and taking the sum of the magnitudes of both resonance lines.

Figure 7 shows the observed distinguishability D_2 for the states $|\Phi(\theta)\rangle$ and $|\Psi(\theta)\rangle$. From Eq. (39), we find the optimal observable $W_1^{(opt)}$ is $\sigma_x^{(1)}$ for $|\Phi(\theta)\rangle$, and $\sin(\kappa)\sigma_x^{(1)}+\cos(\kappa)\sigma_z^{(1)}$ with $\kappa=\arctan[-\sec(\pi/4-\theta/2)]$ for $|\Psi(\theta)\rangle$. Therefore, the transformation R was realized by the NMR pulses $[\pi/2]_{3\pi/2}^1$ and $[\kappa]_{3\pi/2}^1$. As there is no entanglement in the state $|\Phi(\theta)\rangle$, $D_2=\mathcal{P}_2$, while for the entangled state $|\Psi(\theta)\rangle$ we find $D_2>\mathcal{P}_2$. The experimental data also satisfy the relation $D_2^2=\mathcal{P}_2^2+C^2$ of Eq. (9).

V. COMPLEMENTARITY RELATIONS FOR BIPARTITE SYSTEMS

With the same experimental scheme we now explore the complementarity relations for bipartite quantum systems. Between the single-particle visibility $\mathcal{V}_k$ [see Eq. (20)], the two-particle visibility $\mathcal{V}_{12}$ [Eq. (25)], and the predictability $\mathcal{P}_k$ [Eq. (32)], we can verify that the relation

$$\mathcal{V}_{12}^2+\mathcal{V}_k^2+\mathcal{P}_k^2 \leqslant 1 \quad (k=1,2), \tag{41}$$

holds in a pure bipartite system for any experimental setting and measurement basis.

If the initial state $|\Theta\rangle$ has only real coefficients γ_i, the inequality becomes an equality. In this case, the two-particle visibility $\mathcal{V}_{12}$ becomes equal to the concurrence C, $\mathcal{V}_{12}\equiv C=2|\gamma_1\gamma_4-\gamma_2\gamma_3|$. However, when the coefficients γ_i are arbitrary complex numbers, the two-particle visibility $\mathcal{V}_{12}$ can be smaller than the concurrence, $\mathcal{V}_{12}\leqslant C$. As a specific example consider $|\Theta\rangle=-0.3|00\rangle-0.2e^{-i3\pi/5}|01\rangle+0.8e^{-i\pi/25}|10\rangle+0.4796e^{-i5\pi/12}|11\rangle$. Using symmetric beam splitters and the measurement basis $\{|0\rangle,|1\rangle\}$), we find $\mathcal{V}_{12}=0.1627$ and $C=0.2110$, i.e., $\mathcal{V}_{12}<C$.

By the Schmidt decomposition [34], any pure state $|\Theta\rangle$ can be transformed into one with real coefficients by local unitary operations. Therefore, one can design a different experiment using beam splitters that implement the transformation $e^{i\alpha_k/2(\sigma_x^{(k)}\cos\xi_k+\sigma_y^{(k)}\sin\xi_k)}$ instead of the symmetric one $e^{i\pi/4\sigma_y^{(k)}}$. In this case, the single-particle transducers implement the operation

$$U_k(\theta_k,\xi_k,\phi_k) = e^{i\alpha_k/2(\sigma_x^{(k)}\cos\xi_k+\sigma_y^{(k)}\sin\xi_k)}e^{-i\phi_k/2\sigma_z^{(k)}} \tag{42}$$

instead of $U_k(\phi_k)$ in Eq. (10). Note that the single-particle character S_k [Eq. (7)] is invariant under local unitary transformations though its constituents $\mathcal{V}_k$ and $\mathcal{P}_k$ are not. By defining the maximal visibility $V_{12}=\max_{\{\alpha_k,\xi_k\}}\{\mathcal{V}_{12}(\alpha_k,\xi_k)\}$, we obtain $V_{12}\equiv C$ and

$$V_{12}^2+S_k^2=1 \quad (k=1,2). \tag{43}$$

This shows that the complementarity relation (8) in the equality form is fulfilled for any pure bipartite system. An alternative way is to keep the symmetric beam splitters and change the measurement basis. One can always choose an optimal basis which consists of the eigenvectors of an observable $W=W_1\otimes W_2$ that maximizes the visibility $\mathcal{V}_{12}$, i.e., $V_{12}=\max_{\{W\}}\{\mathcal{V}_{12}(W)\}\equiv C$. Being invariant under local unitary transformations, this maximal two-particle visibility V_{12} (= concurrence C) is a good measure of the bipartite property encoded in the pure state.

In a pure bipartite system, the complementarity relation (43), together with the identity $V_{12}\equiv C$ and the definition (7) of the single-particle character S_k offers a method for quantifying entanglement in terms of the directly measurable quantities, in this case visibilities, predictability, and distinguishability. In this section, we experimentally explore these complementarity relations for the states

TABLE I. The various quantities involved in the complementarity relation for the family of states $|\psi(\theta_1,\theta_2)\rangle$ in Eq. (44).

Particle k	$C \equiv V_{12}$	S_k, V_k P_k	D_k
1	$\lvert\sin(\frac{\theta_1-\theta_2}{2})\rvert$	$\lvert\cos(\frac{\theta_1-\theta_2}{2})\rvert$, $\lvert\cos(\frac{\theta_1-\theta_2}{2})\rvert$ 0	$\lvert\sin(\frac{\theta_1-\theta_2}{2})\rvert$
2		$\lvert\cos(\frac{\theta_1-\theta_2}{2})\rvert$, $\lvert\sin(\frac{\theta_1+\theta_2}{2})\cos(\frac{\theta_1-\theta_2}{2})\rvert$ $\lvert\cos(\frac{\theta_1+\theta_2}{2})\cos(\frac{\theta_1-\theta_2}{2})\rvert$	$\sqrt{1-\sin^2(\frac{\theta_1+\theta_2}{2})\cos^2(\frac{\theta_1-\theta_2}{2})}$

$$|\psi(\theta_1,\theta_2)\rangle = \frac{1}{\sqrt{2}}\Bigg[|0\rangle_1 \otimes \left(\cos\frac{\theta_1}{2}|0\rangle_2 + \sin\frac{\theta_1}{2}|1\rangle_2\right) + |1\rangle_1 \otimes \left(\cos\frac{\theta_2}{2}|0\rangle_2 + \sin\frac{\theta_2}{2}|1\rangle_2\right)\Bigg] \tag{44}$$

by preparing the state in the nuclear spins of molecules, and measuring the visibilities, predictability, and distinguishability by NMR according to the procedure outlined above.

Table I lists the theoretical expectations for the various quantities involved in the complementarity relation for this state. The single-particle character S_k and the concurrence C ($\equiv$ the maximal two-particle visibility V_{12}) satisfy the duality relation of Eq. (43). For the state $|\psi(\theta_1,\theta_2)\rangle$ [Eq. (44)], the maximal two-particle visibility V_{12} is obtained from the experimental visibility $\mathcal{V}_{12}$ by setting the measurement basis $\{|x_1y_2\rangle\}$ to the computational basis $\{|x,y=0 \text{ or } 1\rangle\}$. The predictabilities for the two particles are qualitatively different, $P_1 \neq P_2$, which results in $V_1^2+V_{12}^2=1$, whereas $V_2^2+V_{12}^2 \leqslant 1$. The special case with $\theta_1+\theta_2=\pi$ was discussed in detail in Ref. [20]; in that case, both predictabilities vanish, $P_1=P_2=0$. However, $V_{12}^2+V_k^2+P_k^2=1$ and $D_k^2+V_k^2=1$ are still satisfied for $k=1$ or 2.

To verify these relations, we used an experimental procedure similar to that discussed in Sec. III B. To prepare the state $|\psi(\theta_1,\theta_2)\rangle$ from the pseudopure state ρ_{00}, we used the following NMR pulse sequence:

$$|\psi(\theta_1,\theta_2)\rangle: \left[\frac{\pi}{2}\right]_{\pi/2}^{1}\left[\frac{\pi}{2}\right]_{\pi}^{2} - \frac{\theta_1-\theta_2}{2\pi J} - \left[\frac{\pi}{2}\right]_{\pi}^{2}\left[\pi - \frac{\theta_1+\theta_2}{2}\right]_{3\pi/2}^{2}. \tag{45}$$

When $(\theta_1-\theta_2)/2\pi J$ is negative, we generate the required evolution by inserting two π pulses on one of the two qubits before and after the evolution period of $|\theta_1-\theta_2|/2\pi J$.

We measured the visibilities for the state $|\psi(\theta_1,\theta_2)\rangle$ by first scanning ϕ_1 while fixing ϕ_2 to $\pi/2$, then repeated the experiment with fixed ϕ_1 and variable ϕ_2. This provides the maximal probabilities $\bar{p}_{\max,\min}(|x\rangle_1|y\rangle_2)$ of the "corrected" joint probabilities, which occur at $(\phi_1,\phi_2)=(n\pi+\pi/2, m\pi+\pi/2)$ for $|\psi(\theta_1,\theta_2)\rangle$.

As a specific example, we present the experimental results for $|\psi(\theta_1,\theta_2)\rangle$ with $\theta_1+\theta_2=\pi/2$. The resulting interference fringes were closely similar to those shown in Fig. 5. Using the procedure described in Sec. III B, we extracted the relevant visibilities V_k and V_{12} from the experimental data. The visibilities and the predictability were measured as a function of θ_1 varying from $-\pi/4$ to $3\pi/4$ in steps of $\pi/8$. The single-particle character $S_k=\sqrt{V_k^2+P_k^2}$ and the two-particle visibility V_{12} from these experiments are displayed in Fig. 8, together with plots of the theoretical complementarity relations (solid curves) indicating $V_{12}^2+S_k^2=1$ for the pure two-qubit states. A fit of these data to the equation $x^2+y^2=r^2$ resulted in an amplitude $r=0.98\pm0.01$ for the data of Fig. 8(a) and 0.97 ± 0.01 for the data of Fig. 8(b).

For the quantitative measurement of the distinguishability D_k, the optimal observable $W_j^{(opt)}$ for $|\psi(\theta_1,\theta_2)\rangle$ is a spin operator parallel to $\vec{b}=(\sin\kappa,0,\cos\kappa)$ with $\kappa=(\theta_1+\theta_2-\pi)/2$ for D_1, in agreement with Ref. [16], and $\kappa=\arctan(-\cot[(\theta_1+\theta_2)/2]/\sin[(\theta_1-\theta_2)/2])$ for D_2, according to the analysis of Sec. IV B. The transformation R_j was realized by a $[\kappa]_{3\pi/2}^{j}$ pulse. Figure 9 compares the measured values of the single-particle visibilities V_k and the distinguishabilities D_k to the theoretical complementarity relations (solid curves) $D_k^2+V_k^2=1$. The fitted values of the amplitude r are 0.99 ± 0.01 for the data in Fig. 9(a) and 0.98 ± 0.01 for Fig. 9(b).

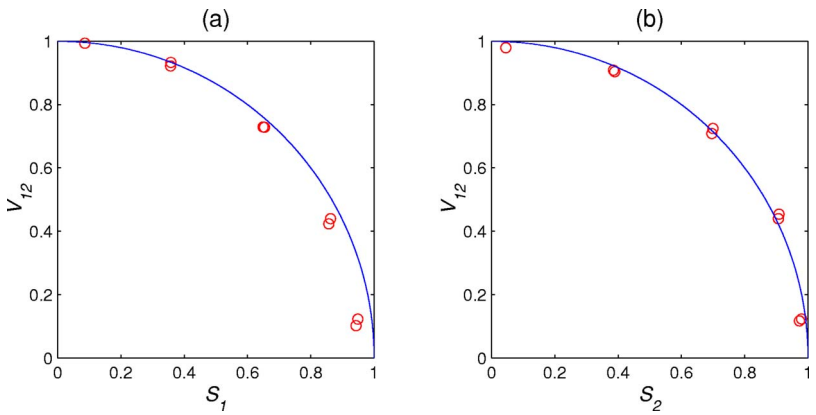

FIG. 8. (Color online) Experimental verification of the complementarity relation $V_{12}^2+S_k^2=1$ in a pure two-qubit system: (a) for qubit 1 and (b) for qubit 2. Solid curves represent the theoretical complementarity relation of single-particle character S_k versus two-particle visibility V_{12}. Experimental results are indicated by circles.

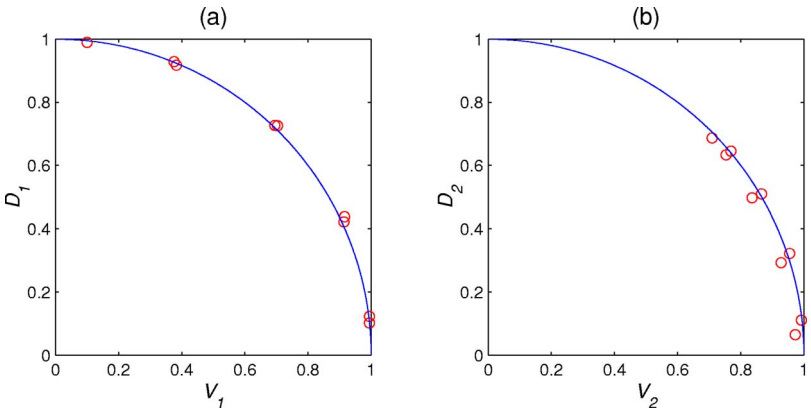

FIG. 9. (Color online) Experimental verification of the complementarity relation of $D_k^2+V_k^2=1$ in a pure two-qubit system. (a) for qubit 1 and (b) for qubit 2. Solid curves represent the ideal complementarity relationship, while experimental results are indicated by circles.

In Fig. 10, we compare two independent ways for measuring the concurrence C, either through the two-particle visibility V_{12}, or through the single-particle quantities, as $\sqrt{D_k^2-P_k^2}$. Both data sets are plotted against θ_1, together with the theoretical concurrence C. The figure shows clearly that the two procedures give the same results, within experimental errors. Apparently, both methods allow one to experimentally determine the entanglement of pure two-qubit states. At the same time, the data verify the complementarity relation (5).

In these experiments, the maximal absolute errors for the quantities V_k, V_{12}, and P_k were about 0.1. The error is primarily due to the inhomogeneity of the radio frequency field and the static magnetic field, imperfect calibration of radio frequency pulses, and signal decay during the experiments. A maximal experimental error about 6% results for the verification of the complementarity relations. If we take into account these imperfections, the measured data in our NMR experiments agree well with the theory.

VI. MULTIQUBIT SYSTEMS

To generalize the complementarity relation (5) to multiqubit systems, we consider a pure state $|\psi\rangle$ with n qubits

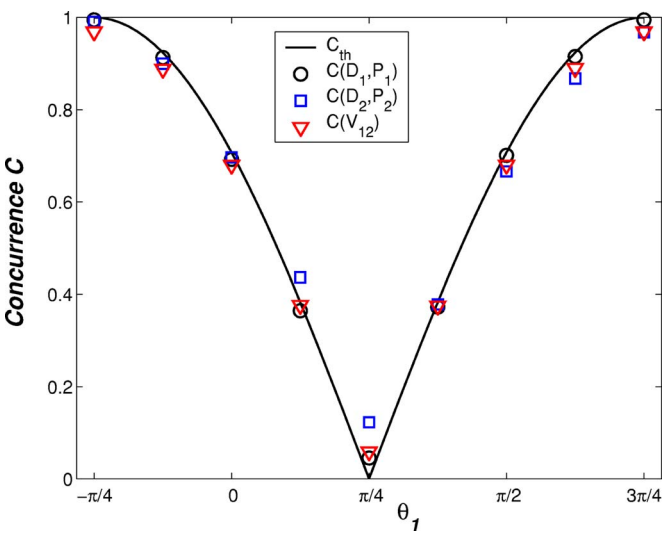

FIG. 10. (Color online) Measured concurrence from the experimental values of V_{12} (denoted by $\triangledown$) and $\sqrt{D_k^2-P_k^2}$ (denoted, respectively, by $\bigcirc$ and $\boxdot$ for $k=1$ and 2) verus θ_1. The solid curve represent the theoretical concurrence $C=|\sin(\theta_1-\pi/4)|$.

$i,j,k,\ldots,m$. According to the generalized concurrence for pairs of quantum systems of arbitrary dimension by Rungta and co-workers [35,36], we calculate the bipartite concurrence $C_{k(ij,\ldots,m)}$ between qubit k and the system with the remaining $n-1$ qubits $(ij,\ldots,m)$ in terms of the marginal density operator ρ_k

$$C_{k(ij,\ldots,m)}=\sqrt{2[1-\mathrm{Tr}(\rho_k^2)]}. \tag{46}$$

In terms of the single-particle character S_k [Eq. (7)], and using $\mathrm{Tr}(\rho_k^2)=\frac{1}{2}(1+S_k^2)$, we obtain the complementarity relation

$$C_{k(ij,\ldots,m)}^2+S_k^2=1. \tag{47}$$

This is a first generalization of the tradeoff between individual particle properties, quantified by S_k, and the bipartite entanglement $C_{k(ij,\ldots,m)}$ to many particle systems. It implies also the relation $\Sigma_{i=1}^n[C_{k(ij,\ldots,m)}^2+S_k^2]=n$ derived by Tessier [26].

To characterize the pairwise entanglements of qubit k with the other qubits, we sum over the squares of the concurrences of all two-partite subsystems involving qubit k,

$$\tau_2^{(k)}=\sum_{j\neq k}C_{kj}^2. \tag{48}$$

Here, the concurrence C_{kj} is defined in terms of the marginal density operator ρ_{kj} for the kj subsystem, using the definition of $C(\rho_{kj})=\max\{\lambda_1-\lambda_2-\lambda_3-\lambda_4,0\}$, where $\lambda_i(i=1,2,3,4)$ are the square roots of the eigenvalues of $\rho_{kj}(\sigma_y^{(k)}\sigma_y^{(j)})\rho_{kj}^*(\sigma_y^{(k)}\sigma_y^{(j)})$ in decreasing order [28,29].

We now specialize to pure three-qubit systems. Here, it is possible to specify three-partite entanglement by the 3-tangle τ_3 [37] as

$$\tau_3=C_{k(ij)}^2-C_{ki}^2-C_{kj}^2. \tag{49}$$

Combining Eqs (47)–(49), we find a complementarity between single-particle properties S_k, pair-wise entanglement $\tau_2^{(k)}$, and three-partite entanglement τ_3, which is valid for each individual qubit:

$$\tau_3+\tau_2^{(k)}+S_k^2=1. \tag{50}$$

For specific examples, we have listed in Table II different three-qubit states and calculated the one-, two-, and three-qubit quantifiers appearing in Eq. (50). As can be verified

TABLE II. Some examples for the complementarity relation $\tau_3+\tau_2^{(k)}+S_k^2=1$ in a pure three-qubit system.

Class	τ_3	$\tau_2^{(k)}$	$S_k^2=V_k^2+P_k^2$
Product states	0	0	1
Bipartite entanglement $\|\psi_{r-st}\rangle=\|0\rangle_r(a_1\|00\rangle+a_2\|11\rangle)_{st}$	0	$0,(k=r)$ $4\|a_1a_2\|^2,(k=s,t)$	$1,(k=r)$ $(\|a_1\|^2-\|a_2\|^2)^2,(k=s,t)$
W states $\|W\rangle=a_1\|001\rangle+a_2\|010\rangle+a_3\|100\rangle$	0	$\sum_{j\neq k}4\|a_ka_j\|^2$	$(\|a_k\|^2-\sum_{j\neq k}\|a_j\|^2)^2$
GHZ states $\|GHZ\rangle=a_1\|000\rangle+a_2\|111\rangle$	$4\|a_1a_2\|^2$	0	$(\|a_1\|^2-\|a_2\|^2)^2$

from the table, these states satisfy Eq. (50) in different ways. The product states of the first entry only have single-particle character. As discussed by Dür *et al.* [38], the states listed in the second entry represent bipartite entanglement between the second and third qubit, while the first qubit is in a product state with them. The GHZ states are pure three-particle entangled states, while the W states exhibit no *genuine* three-particle entanglement, but two- and one-particle properties.

Since there is no generalization of the 3-tangle to larger systems, we can only speculate here if it is possible to extend the relation (50) to more than three qubits. On a heuristic basis, we consider two types of pure n-qubit systems. One is a generalization of the GHZ states to n qubits: $|GHZ_n\rangle=a_1|0\rangle^{\otimes n}+a_2|1\rangle^{\otimes n}$. This is a state with pure n-way entanglement, i.e.,

$$\tau_n=4|a_1a_2|^2,\quad \tau_m^{(k)}=0 \text{ for } 1<m<n$$

$$S_k^2=(|a_1|^2-|a_2|^2)^2, \tag{51}$$

where $\tau_m^{(k)}$ denotes the *pure* m-tangle regarding qubit k. Here, the m-tangle denotes m-way or m-party entanglement that critically involves all m parties, which is different from the I tangle in Ref. [35,36] and a recently introduced measure of multipartite entanglement defined by $C_{(n)}^2=\mathrm{Tr}(\rho\tilde{\rho})$ with a spin-flip operation $\tilde{\rho}\equiv\sigma_y^{\otimes n}\rho\sigma_y^{\otimes n}$ by Wong and Christensen [39]. Currently, there is no general way to measure this form of entanglement beyond three qubits.

The W states of Table II may also be generalized to n qubits as $|W_n\rangle=a_1|100\ldots0\rangle+a_2|010,\ldots0\rangle+a_3|001,\ldots,0\rangle+\cdots++a_n|000\ldots1\rangle$. These states exhibit the maximal bipartite entanglements and no other m-way entanglements, i.e.,

$$\tau_m^{(k)}=0 \text{ for } 2<m\leqslant n,\quad \tau_2^{(k)}=\sum_{j\neq k}4|a_ka_j|^2$$

$$S_k^2=\left(|a_k|^2-\sum_{j\neq k}|a_j|^2\right)^2. \tag{52}$$

In these two cases the complementarity relation generalizes to $\Sigma_{m=2}^n\tau_m^{(k)}+S_k^2=1$.

VII. CONCLUSIONS

Complementarity is a universal relationship between properties of quantum objects. However, it behaves in different ways for different quantum objects. The purpose of this paper was to analyze the different complementarity relations that exist in two- and multiqubit systems and to illustrate some of them in a simple NMR system.

We experimentally verified the complementarity relation between the single-particle and bipartite properties: $C^2+S_k^2=1$ in a pure two-qubit system. To determine the entanglement, we used either the two-particle visibility V_{12} or the distinguishability D_k and the predictability P_k. Accordingly, two complementarity relations: $V_{12}^2+V_k^2+P_k^2=1$ and $D_k^2+V_k^2=1$ were tested for different states including maximally entangled, separable, as well as partially entangled (intermediate) states.

Furthermore, the complementarity $C^2+S_k^2=1$ between one- and two-particle character was generalized to systems of n qubits. The complementarity relation $C_{k(ij,\ldots,m)}^2+S_k^2=1$ holds for an arbitrary pure n-qubit state, which implies a tradeoff between the *local* single-particle property $(S_k^2=V_k^2+P_k^2)$ and the *nonlocal* bipartite entanglement between the particle and the remainder of the system $(C_{k(ij,\ldots,m)}^2)$. More interesting, in a pure three-qubit system, the single-particle character (S_k^2), the two-particle property regarding this particle measured by the sum of all pair-wise entanglements involving the particle $(\tau_2^{(k)})$, and the three-particle property measured by the *genuine* tripartite entanglement (τ_3) are complementary, i.e., $\tau_3+\tau_2^{(k)}+S_k^2=1$. However, the generalization of the similar relationship to a larger-qubit system requires the identification and quantification of multipartite entanglement for pure and mixed states beyond three-qubit systems that still remains an open question currently. A similar relationship cannot be directly generalized to larger qubit systems. Some specific samples might be helpful to conjecture the relation $\Sigma_{m=2}^n\tau_m^{(k)}+S_k^2=1$: the single-particle property (*local*) of a particle might be complementary to all possible *pure* multiparticle properties (*nonlocal*) connected to this particle.

Complementarity and entanglement are two important phenomena that characterize quantum mechanics. From these observations, we conclude that entanglement in its various forms is an important parameter for the different forms of complementarity relations in multipartite systems. Different forms of entanglement quantify the amount of information encoded in the different quantum correlations of

the system, indicating the multipartite quantum attributes. These results have also implications on the connection between entanglement sharing and complementarity and maybe in turn provide a possible way to study the entanglement in multipartite quantum systems by complementarity. We hope that these findings will be useful for future research into the nature of complementarity and entanglement.

ACKNOWLEDGMENTS

We thank Reiner Küchler for help with the experiments. X. Peng acknowledges support by the Alexander von Humboldt Foundation. This work is supported by the National Natural Science Foundation of China (Grant Nos. 10274093 and 10425524) and by the National Fundamental Research Program (Grant No. 2001CB309300).

[1] N. Bohr, Naturwiss. **16**, 245 (1928); Nature (London) **121**, 580 (1928).
[2] R. P. Feynman, R. B. Leifhton, and M. Sands, *Quantum Mechanics*, The Feynamn Lectures of Physics Vol. III (Addison-Wesley, Reading, 1965).
[3] M. O. Scully, B.-G. Englert, and H. Walther, Nature (London) **351**, 111 (1991).
[4] K. Simonyi, *Kulturgeschichte der Physik* (Verlag Harri Deutsch, Thun, 1990).
[5] W. K. Wootters and W. H. Zurek, Phys. Rev. D **19**, 473 (1979); L. S. Bartell, *ibid.* **21**, 1698 (1980); D. M. Greenberger and A. Yasin, Phys. Lett. A **128**, 391 (1988); L. Mandel, Opt. Lett. **16**, 1882 (1991).
[6] L. S. Bartell, Phys. Rev. D **21**, 1698 (1980).
[7] D. M. Greenberger and A. Yasin, Phys. Lett. A **128**, 391 (1988).
[8] L. Mandel, Opt. Lett. **16**, 1882 (1991).
[9] G. Jaeger, A. Shimony, and L. Vaidman, Phys. Rev. A **51**, 54 (1995).
[10] B.-G. Englert, Phys. Rev. Lett. **77**, 2154 (1996); B.-G. Englert, and J. A. Bergou, Opt. Commun. **179**, 337 (2000).
[11] G. I. Taylor, Proc. Cambridge Philos. Soc. **15**, 114 (1909); P. Mittelstaedt, A. Prieur, and R. Schieder, Found. Phys. **17**, 891 (1987); P. D. D. Schwindt, P. G. Kwiat, and B.-G. Englert, Phys. Rev. A **60**, 4285 (1999).
[12] G. Möllenstedt and C. Jönsson, Z. Phys. **155**, 472 (1959); A. Tonomura, J. Endo, T. Matsuda, and T. Kawasaki, Am. J. Phys. **57**, 117 (1989).
[13] A. Zeilinger, R. Gähler, C. G. Shull, W. Treimer, and W. Mampe, Rev. Mod. Phys. **60**, 1067 (1988); H. Rauch and J. Summhammer, Phys. Lett. **104**, 44 (1984); J. Summhammer, H. Rauch, and D. Tuppinger, Phys. Rev. A **36**, 4447 (1987).
[14] O. Carnal and J. Mlynek, Phys. Rev. Lett. **66**, 2689 (1991); S. Dürr, T. Nonn, and G. Rempe, *ibid.* **81**, 5705 (1998); P. Bertet, S. Osnaghl, A. Rauschenbeutel, G. Nogues, A. Auffeves, M. Brune, J. M. Ralmond, and S. Haroche, Nature (London) **411**, 166 (2001).
[15] X. Zhu, X. Fang, X. Peng, M. Feng, K. Gao, and F. Du, J. Phys. B **34**, 4349 (2001).
[16] X. Peng, X. Zhu, X. Fang, M. Feng, M. Liu, and K. Gao, J. Phys. A **36**, 2555 (2003).
[17] R. Ghosh and L. Mandel, Phys. Rev. Lett. **59**, 1903 (1987).
[18] C. O. Alley and Y. H. Shih, in *Proceedings of the Second International Symposium on Foundations of Quantum Mechanics in Light of New Technology*, edited by M. Namiki *et al.* (Physical Society of Japan, Tokyo, 1986), p. 47; Y. H. Shih and C. O. Alley, Phys. Rev. Lett. **61**, 2921 (1988); C. K. Hong, Z. Y. Ou, and L. Mandel, *ibid.* **59**, 2044 (1987); J. G. Rarity and P. R. Tapster, *ibid.* **64**, 2495 (1990); P. G. Kwiat, W. A. Vareka, C. K. Hong, H. Nathel, and R. Y. Chiao, Phys. Rev. A **41**, R2910 (1990); M. Horne, A. Shimony, and A. Zeilinger, in *Quantum Coherence*, edited by J. Anandan (World Scientific, Singapore, 1990), p. 356.
[19] M. A. Horne and A. Zeilinger, in *Proceedings of the Symposium on the Foundations of Modern Physics*, edited by P. Lahti and P. Mittelstaedt (World Scientific, Singapore, 1985), p. 435.
[20] G. Jaeger, M. A. Horne, and A. Shimony, Phys. Rev. A **48**, 1023 (1993).
[21] A. F. Abouraddy, M. B. Nasr, B. E. A. Saleh, A. V. Sergienko, and M. C. Teich, Phys. Rev. A **63**, 063803 (2001).
[22] J. Oppenheim, K. Horodecki, M. Horodecki, P. Horodecki, and R. Horodecki, Phys. Rev. A **68**, 022307 (2003).
[23] B. E. A. Saleh, A. F. Abouraddy, A. V. Sergienko, and M. C. Teich, Phys. Rev. A **62**, 043816 (2000).
[24] S. Bose and D. Home, Phys. Rev. Lett. **88**, 050401 (2002).
[25] G. Jaeger, A. V. Sergienko, B. E. A. Saleh, and M. C. Teich, Phys. Rev. A **68**, 022318 (2003).
[26] T. E. Tessier, Found. Phys. Lett. **18**, 107 (2005).
[27] M. Jakob and J. A. Bergou, arXiv: eprint quant-ph/0302075 (unpublished).
[28] W. K. Wootters, Phys. Rev. Lett. **80**, 2245 (1998).
[29] W. K. Wootters, Quantum Inf. Comput. **1**, 27 (2001).
[30] D. Suter, K. T. Mueller, and A. Pines, Phys. Rev. Lett. **60**, 1218 (1988).
[31] D. G. Cory, A. F. Fahmy, and T. F. Havel, Proc. Natl. Acad. Sci. U.S.A. **94**, 1634 (1997); N. A. Gershenfeld and I. L. Chuang, Science **275**, 350 (1997).
[32] G. Brassard, S. Braunstein, and R. Cleve, Phys. Dokl. **120**, 43 (1998).
[33] G. Teklemariam, E. M. Fortunato, M. A. Pravia, T. F. Havel, and D. G. Cory, Phys. Rev. Lett. **86**, 5845 (2001).
[34] M. A. Nielsen and I. L. Chuang, *Quantum Computation and Quantum Information* (Cambridge Univ. Press, Cambridge, 2000).
[35] P. Rungta and C. M. Caves, Phys. Rev. A **67**, 012307 (2003).
[36] P. Rungta, V. Buzek, C. M. Caves, M. Hillery, and G. J. Milburn, Phys. Rev. A **64**, 042315 (2001).
[37] V. Coffman, J. Kundu, and W. K. Wootters, Phys. Rev. A **61**, 052306 (2000).
[38] W. Dür, G. Vidal, and J. I. Cirac, Phys. Rev. A **62**, 062314 (2000).
[39] A. Wong and N. Christensen, Phys. Rev. A **63**, 044301 (2001).